Weighting Nitrogen and Phosphorus Pixel Pollutant Loads to Represent Runoff and Buffering Likelihoods

2 authors:

Emily Stephan
NYC Parks

3 PUBLICATIONS   **9** CITATIONS

SEE PROFILE

Theodore A. Endreny
State University of New York College of Environmental Science and Forestry

142 PUBLICATIONS   **1,641** CITATIONS

SEE PROFILE

Some of the authors of this publication are also working on these related projects:

Urban forest models of ecosystem functions that reduce pollution View project

Hydrodynamics, morphodynamics, stratigraphy, sediment transport and mixing about a large confluence in the Amazon Basin View project

WEIGHTING NITROGEN AND PHOSPHORUS PIXEL POLLUTANT LOADS TO REPRESENT RUNOFF AND BUFFERING LIKELIHOODS[1]

Emily A. Stephan and Theodore A. Endreny[2]

ABSTRACT: Watershed models often estimate annual nitrogen (N) or phosphorus (P) pollutant loads in rural areas with export coefficient (EC) (kg/ha/yr) values based on land cover, and in urban areas as the product of spatially uniform event mean concentration (EMC) (mg/L) values and runoff volume. Actual N and P nonpoint source (NPS) pollutant loading has more spatial complexity due to watershed variation in runoff likelihood and buffering likelihood along surface and subsurface pathways, which can be represented in a contributing area dispersal area (CADA) NPS model. This research develops a CADA NPS model to simulate how watershed properties of elevation, land cover, and soils upslope and downslope of each watershed pixel influence nutrient loading. The model uses both surface and subsurface runoff indices (RI), and surface and subsurface buffer indices (BI), to quantify the runoff and buffering likelihood for each watershed pixel, and generate maps of weighted EC and EMC values that identify NPS pollutant loading hotspots. The research illustrates how CADA NPS model maps and pixel loading values are sensitive to the spatial resolution and accuracy of elevation and land cover data, and model predictions can represent the lower and upper bounds of NPS loading. The model provides managers with a tool to rapidly visualize, rank, and investigate likely areas of high nutrient export.

(KEY TERMS: nonpoint source pollution; watershed management; nutrients; runoff; land use/land cover change; urbanization.)

INTRODUCTION

Nonpoint source (NPS) pollution is a pervasive water quality problem around the world, delivering excess nitrogen (N) and phosphorus (P) nutrients to rivers, lakes, and estuaries and causing cultural, or accelerated, eutrophication with excessive plant and algae growth (Carpenter *et al.*, 1998; Kaushal *et al.*, 2011). Cultural eutrophication due to N and P runoff

from human activities is the primary impairment facing most surface waters today (Smith and Schindler, 2009). To address this impairment and improve aquatic ecosystem health, watershed management programs often seek to identify and then reduce human generated N and P loading (Conley *et al.*, 2009; Lewis *et al.*, 2011). Management for NPS runoff must consider that some loading of N and P is required to support aquatic plant and algae growth, and the relative abundance of these limiting nutrients in rivers, lakes,

and estuaries is what triggers cultural eutrophication (Conley *et al.*, 2009). Concentrated human activities within urban areas represents a unique problem, both generating complex sources and elevated magnitudes of N and P pollutant runoff (Kaye *et al.*, 2006) and diminishing interaction between runoff and vegetated land cover that provide nutrient sinks through filtration and transformation (Bettez and Groffman, 2012). Watershed water quality models can assist with NPS identification nutrient loading hotspots, but must balance model accuracy and complexity with data availability and feasibility (e.g., Borah and Bera, 2004; Zhang *et al.*, 2012).

Urban managers seeking spatially distributed, rainfall-runoff watershed models to identify NPS hotspots and predict receiving water loading of N and P often model mixed-use watersheds, comprised of urban, agricultural, and forested land covers. A variety of tools are available for urban runoff simulation, including the U.S. Environmental Protection Agency (USEPA) SWMM (stormwater management model) (Huber, 1995), RHESSys (Regional Hydro-Ecologic Simulation System) (Tague and Band, 2004), and U.S. Department of Agriculture (USDA) i-Tree Hydro (Wang *et al.*, 2008). SWMM simulates the routing of pervious and impervious runoff from user-defined subwatersheds into storm sewers, with the option for the user to insert a best management practice upstream of the storm sewer. The SWMM tool does not use elevation and land cover data to predict runoff pathways and the intersection of runoff, pollutants, and filtration, but instead has the user define connections between runoff sources, treatments, and sinks. RHESSys is a continuous simulation, spatially-distributed tool using advanced governing equations to represent the hydrologic budget within a spatially distributed geographic information system (GIS) representation of watershed elevation and land cover data, operating at a daily time step to predict runoff generation, flow paths, and N nutrient processes (Tague and Band, 2004). This tool is typically applied to highly instrumented watersheds, requiring extensive parameterization, and might be considered a higher order model. By contrast, the i-Tree Hydro (v5) model is a continuous simulation, statistically-distributed first order, or parsimonious, model of the hydrologic budget, using the basic governing equations to predict the distribution of soil saturation and runoff response to rainfall and snowfall for each hydrologically similar area, defined by the topographic index (Beven and Kirkby, 1979). The i-Tree Hydro model uses nationally available datasets with a database of location data, including leaf on and off dates, to represent the influence of elevation, soils, and vegetation on saturation excess and infiltration excess runoff (Wang *et*

al., 2008). The i-Tree Hydro model, like SWMM, combines the total surface runoff with event mean concentration (EMC) values (mg/L) to simulate the NPS pollutant load entering receiving waters.

Simulation of rural watershed areas should account for agricultural and forest land cover, and popular continuous simulation, spatially distributed models include the USDA's SWAT (Soil Water Assessment Tool) (Douglas-Mankin *et al.*, 2010), USEPA's HSPF (Hydrologic Simulation Program — Fortran) (Donigian *et al.*, 1995), and AgNPS (Agricultural NonPoint Source) (Young *et al.*, 1989), each developed more than 30 years ago. While these models can represent the spatial heterogeneity of land cover, only AgNPS simulates the effect of runoff flow paths on changes in water quality, with user defined flow paths establishing connectivity between land use types (Fisher *et al.*, 1997). An alternative to the higher order, extensively parameterized models (e.g., SWAT, HSPF, AgNPS) is the first order, empirical Export Coefficient model which estimates the watershed annual NPS load of N or P, and can use GIS to map and sum the product of land cover type area and the export coefficient (EC) value (kg/ha/yr) specified for each land cover type (Reckhow *et al.*, 1980; Reckhow and Simpson, 1980). The EC model was combined with theory of variable source area hydrology and vegetative filtering of nutrients in the contributing area and dispersal area (CADA) model (Endreny and Wood, 2003). The CADA model used biophysical algorithms to auto-calculate flow paths surrounding each pixel EC value; runoff from the pixel was given a likelihood based on the topographic index, which is the quotient of the contributing area and pixel slope while filtering below the pixel was given a likelihood based on a buffering index, which is the quotient of dispersal area and flow path slope through land cover types known to buffer NPS pollution.

The CADA EC model predicted which watershed pixels were P loading hotspots using existing terrain and land cover maps and a regional EC dataset. For each land cover pixel, the product of runoff likelihood, buffer likelihood, and EC value provided a weighted EC value, which was mapped across the watershed and summed to provide the total watershed P load (Endreny and Wood, 2003). While the CADA EC model could rapidly identify potential hotspots of P loading, it was not extended to simulate N loading, EMC loads from urban areas, the difference between impervious and pervious runoff likelihood, or the difference in buffer likelihood along subsurface *vs.* surface flow paths, which are important characteristics of mixed-use watersheds.

This article presents an enhanced CADA NPS model that includes: (1) flexibility to use EC, EMC

or other NPS loading data for N or P loads; (2) representation of impervious and pervious runoff paths in the contributing area; and (3) representation of surface and subsurface buffer paths in the dispersal. In the methods section the model algorithms and data sources are introduced, and in the results section a sensitivity test is examined that explains model response to differences in the horizontal resolution of the terrain and land cover inputs that are critical in contributing and dispersal area calculations.

MATERIALS AND METHODS

Site Description

The watershed used for this study is delineated from Onondaga Creek at Spencer Street (USGS gage 02420010, located at 43°03′27″, −76°09′45″) and it drains south to north, with headwaters in the Appalachian Plateau reaching an elevation of 587 m, its outlet in the City of Syracuse at an elevation of 110 m (Figure 1). The watershed has an area of 298 km^2, of which 53 km^2 is classified as developed, and an area of 24.1 km^2 held as sovereign land by the people of the Onondaga Nation. Based on the 2006 National Land Cover Database (NLCD) impervious surface maps, only 6% of the study area is designated as impervious cover, and this is concentrated near the northern watershed outlet (see NLCD classes 21, 22, 23, and 24 in Figure 1). The annual average precipitation for Syracuse, New York, is 96.5 cm depth, with an average annual liquid equivalent snowfall of 32 cm, and average monthly total precipitation ranging between 8.1 and 10.4 cm. The average annual air temperature is 9.1°C with a February average low of −8.3°C and July average high of 27.8°C. Flow in Onondaga Creek is regulated by an earthen dam near the northern edge of Onondaga Nation land, designed to allow nonflood flows to pass at grade with the channel bed through a 2 m diameter concrete culvert; when floods fill the reservoir behind the dam the culvert constrains maximum discharge to 36 m^3/s.

Model Structure

The enhanced CADA NPS model is built upon the framework of Endreny and Wood (2003) to create a map of watershed runoff likelihood and buffer likelihood values using publicly available GIS inputs,
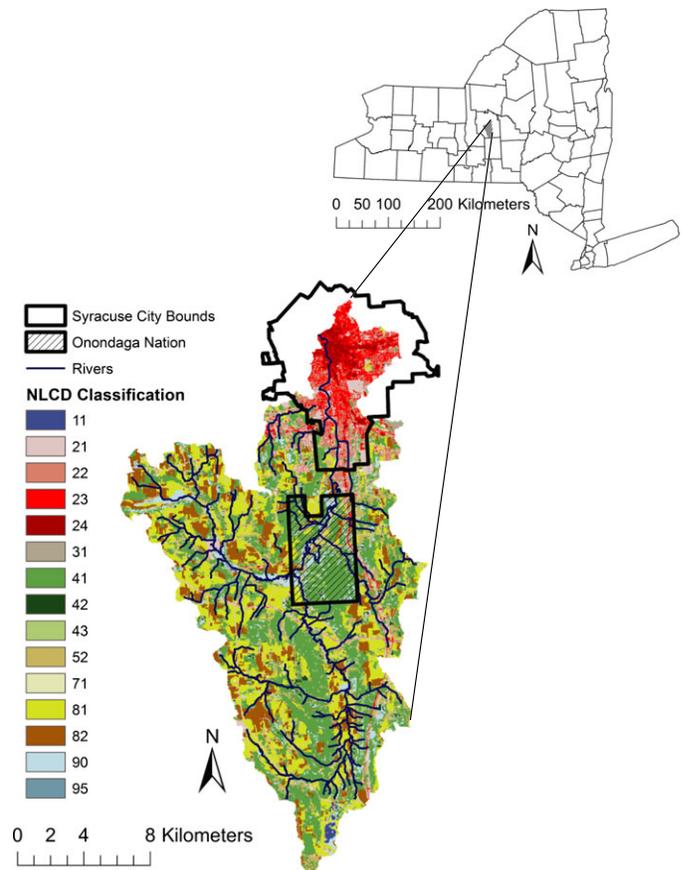
FIGURE 1. Site Map for Onondaga Creek Watershed at Spencer St. National Land Cover Database (NLCD).

which include digital elevation model (DEM) data, NLCD, Soil Survey Geographic (SSURGO) data, as well as annual rainfall data and look-up tables of EC and EMC NPS values. The enhanced CADA model: (1) calculates separate urban and rural NPS pollutant loads for each pixel, using ECs on rural pixels and EMCs on urban pixels; (2) calculates a separate surface and subsurface runoff index (RI) for each pixel based on the fraction of imperviousness and perviousness in each upslope pixel, which is related to an estimate of surface and subsurface wetness; and (3) calculates a separate surface and subsurface buffer index (BI) for each pixel based on flow resistance and potential energy, which is related to runoff velocity and an estimate of NPS buffering. The entire set of pixel specific RI and BI values are normalized to the watershed mean RI and BI values (or median values, depending on user preference), and multiplied by the land cover NPS load to quantify pollutant loading likelihood, which will range from relatively high to low across the watershed. The updated CADA NPS equations calculate weighted surface and subsurface NPS loads for each pixel i, NPS$_{surf,i,weighted}$ and NPS$_{sub,i,weighted}$ as:

$$\text{NPS}_{\text{surf,i,weighted}} = \text{NPS}_{\text{surf,i}} \times \frac{\text{RI}_{\text{surf,i}}}{\text{RI}_{\text{surf,avg}}} \times \frac{\text{BI}_{\text{surf,avg}}}{\text{BI}_{\text{surf,i}}}$$

$$(1)$$

$$\text{NPS}_{\text{sub,i,weighted}} = \text{NPS}_{\text{sub,i}} \times \frac{\text{RI}_{\text{sub,i}}}{\text{RI}_{\text{sub,avg}}} \times \frac{\text{BI}_{\text{sub,avg}}}{\text{BI}_{\text{sub,i}}}$$

$$(2)$$

where NPS_i represents the unweighted NPS load (kg/ha/yr) for land cover type i, RI_i is the pixel's surface or subsurface runoff index value, the RI_{avg} is the corresponding average surface or subsurface runoff index in the watershed, the BI_i is the pixel's surface or subsurface buffer index value, and BI_{avg} is the corresponding average surface or subsurface buffer index in the watershed. The RI and BI terms in Equation (1) use algorithms specific to subsurface and surface runoff and buffer processes.

Urban and Rural, Surface and Subsurface Pollutant Loads

Land cover EC values (kg/ha/yr) were obtained from a local Onondaga Creek study (Coon and Reddy, 2008) as well as from a range of nationally reported values (see Table 1), while EMC values (mg/L) were obtained from the i-Tree Hydro model, which compiled data from the USEPA and others (USEPA, 1983) (Table 1). The NPS pollutant of P was simulated as total phosphorus entrained in surface runoff processes, denoted as $\text{NPS}_{\text{surf,i}}$ in Equation (1). The NPS pollutant of N was simulated as dissolved nitrate in subsurface runoff processes, denoted as $\text{NPS}_{\text{sub,i}}$ in Equation (2).

EMC values (mg/L) were converted into mass per hectare per year loads NPS_i (kg/ha/yr) by taking the product of the EMC value and estimated annual runoff depth (m), and accounting for unit conversions. The annual runoff depth was determined using a modified version of the USEPA Simple Method:

$$\text{NPS}_i = 10{,}000 \times P \times P_j \times R_v \times \text{EMC}_i \qquad (3)$$

where NPS_i represents the pixel i pollutant load (kg/ha/yr), 10,000 is a unit conversion factor, P is annual rainfall (m), P_j is fraction of annual rainfall events that cause runoff (default is 0.9), R_v is the runoff coefficient, and EMC_i is the pixel i pollutant concentration (mg/L). Uniform EMC values of 0.266 mg/L for TP and 0.666 mg/L for nitrate were used on each developed NLCD class 21-24, which range from low to high intensity developed and are concentrated in the city limits (Figure 1); the choice of uniform values is in keeping with USEPA Nationwide Urban Runoff Program (NURP) findings (USEPA, 1983). EMC values for a range of land uses can be found in Table 2; we have chosen to use uniform EMC values reported above due to the lack of statistical difference between land use types. The CADA model predicts variation in EMC derived loads (e.g., NPS_i) due to variation in the R_v, which were set based on the fraction of pixel imperviousness (I_a), where $R_v = 0.05 + 0.9(I_a)$ (Schueler, 1987).

The EMC values reported by NURP are lognormally distributed, so we can determine the 10th (Equation 4) and 90th (Equation 5) percentile values to get a range of low to high EMC estimates:

TABLE 1. Export Coefficient Table.

NLCD Class	Land Use Description	Area (ha)	Locally Derived EC Value — TP (kg/ha/yr)	Locally Derived EC Value — Nitrate (kg/ha/yr)	EC TP Range (kg/ha/yr)	EC Nitrate Range (kg/ha/yr)
11	Open water	86	0.00	0.00	—	—
21	Developed, open Space	1,876	0.86	1.79	—	—
22	Developed, low intensity	1,626	0.54	2.35	—	—
23	Developed, medium intensity	1,251	0.54	2.35	—	—
24	Developed, high intensity	513	1.15	4.93	—	—
31	Barren land (rock/sand/clay)	66	0.86	1.79	0.19-6.23	0.49-3.0
41	Deciduous forest	9,132	0.10	3.70	0.019-0.830	0.59-4.6
42	Evergreen forest	312	0.10	3.70	0.019-0.830	0.59-4.6
43	Mixed forest	728	0.10	3.70	0.019-0.830	0.59-4.6
52	Shrub/scrub	2,798	0.10	3.70	0.019-0.830	0.59-4.6
71	Grassland/herbaceous	183	0.10	3.70	0.019-0.830	0.59-4.6
81	Pasture/hay	6,163	0.28	6.50	0.14-4.90	4.6-20.4
82	Cultivated crops	3,185	2.37	12.44	0.10-18.6	4.6-20.4
90	Woody wetlands	1,835	0.05	0.34	0.05-0.21	—
95	Emergent herbaceous wetlands	83	0.05	0.34	0.05-0.21	—

TABLE 2. Median Event Mean Concentrations for Urban Land Uses (U.S. Environmental Protection Agency, Washington, D.C., 1983).

Pollutant	Units	Residential	Mixed	Commercial	Open/Nonurban
BOD	mg/L	10	7.8	9.3	—
COD	mg/L	73	65	57	40
TSS	mg/L	101	67	69	70
Total lead	µg/L	144	114	104	30
Total copper	µg/L	33	27	29	—
Total zinc	µg/L	135	154	226	195
Total Kjeldahl nitrogen	µg/L	1,900	1,288	1,179	965
Nitrate + nitrite	µg/L	736	558	572	543
Total phosphorus	µg/L	383	263	201	121
Soluble phosphorus	µg/L	143	56	80	26

Note: BOD, biochemical oxygen demand; COD, chemical oxygen demand; TSS, total suspended solids.

$$10_x = \exp(\ln(50_x + z_10 * \sigma)) \tag{4}$$

$$90_x = \exp(\ln(50_x + z_90 * \sigma)) \tag{5}$$

where 50_x is the median EMC value, z is the z-score corresponding to the desired percentile, and σ is the standard deviation for the distribution (in this case, both nitrate and phosphorus had σ ranging from 0.5 to 1, so 0.75 was used).

Runoff Indices — Surface and Subsurface

Surface Runoff Index. The surface runoff index, $RI_{surf,i}$, is based on the topographic index equation for saturation likelihood (Beven and Kirby, 1979), which was modified to only accumulate for each pixel i its upslope area in impervious cover:

$$RI_{surf,i} = \ln\left(\frac{FA_{imp,i}}{S_{surf,i}}\right) \tag{6}$$

where $FA_{imp,i}$ is the flow accumulation of impervious area per pixel width, $S_{surf,i}$ is the local pixel surface terrain slope (tan ß, where ß is in degrees). $FA_{imp,i}$ was computed with the ArcGIS flow accumulation function, which uses a flow direction grid, derived from the DEM, to determine the upslope pixels that drain to the local pixel i, and a weighting grid of scalar values that will be accumulated, or summed, within the upslope area. For $FA_{imp,i}$ the weighting grid was set to total impervious area per pixel width; e.g., an upslope pixel with 10 m × 10 m sides has a contour width of 10 m, and if it had 85% impervious cover, it would contribute 8.5 m = [10 m × 10 m × 0.85 m]/10 m.

Subsurface Runoff Index. The subsurface runoff index, $RI_{sub,i}$ is based on the soil topographic index equation for saturation likelihood (Sivapalan *et al.*, 1987), which was modified to only accumulate for each pixel i its upslope area in pervious cover:

$$RI_{sub,i} = \ln\left(\frac{T_{avg}FA_{per,i}}{T_iS_{sub,i}}\right) \tag{7}$$

where T_{avg} is the mean transmissivity (m²/day) of the watershed and T_i is the transmissivity of the specific cell, where transmissivity is defined as the product of watertable depth and hydraulic conductivity, $FA_{per,i}$ is the flow accumulation of pervious area per pixel width, and $S_{sub,i}$ is the local subsurface watertable slope (tan ß, where ß is in degrees). The pixel impervious cover fraction, and its compliment of pervious cover fraction, was provided by NLCD 2006 data. The pixel transmissivity was provided by SSURGO data; pixels without SSURGO data, such as the Onondaga Nation in our study area, set $T_i = T_{avg}$.

Buffering Indices — Surface and Subsurface

Surface Buffering Index. The surface buffering index is derived as the inverse of travel time from the source pixel to the receiving water, along a lateral surface flow path that follows the terrain slopes. Travel time is derived as the quotient of travel length and velocity:

$$\tau_{surf,i} = \frac{l_i}{V_{surf,i}} \tag{8}$$

where l (m) is travel path distance across pixel i, and V_{surf} (m/s) is the surface runoff velocity for pixel i, computed with the Manning equation:

$$V_{surf} = \frac{C_m}{n}R^{2/3}S^{1/2} \tag{9}$$

where C_m is the Manning coefficient of 1 for SI units (1.486 for BG units), R is the hydraulic radius (m) of flow depth, which varies by land cover (Wurbs and James, 2002; Table 8.1), S is the slope (tan ß, where ß

is slope angle) of the surface pixel, and n is the Manning roughness coefficient (unitless; Table 1, Engman, 1986; Wurbs and James, 2002). The $\tau_{surf,i}$ is set to 0 for all surface water pixels, which are considered receiving waters that have no buffering. The surface buffering index is then calculated as the flow accumulation of travel times for all pixels in the dispersal area:

$$BI_{surf} = FA_{\tau_{surf,i}} \qquad (10)$$

where $FA_{\tau_{surf,i}}$ uses a flow direction grid derived from a negated DEM (i.e., relatively large positive elevations along ridges become large negative elevations, lower than those of relatively small negative elevations within valleys), and a weighting grid of $\tau_{surf,i}$. The BI_{surf} calculation is based on longer travel times equating to greater chances for pollutant removal through a range of biophysical processes, such as particle settling, filtration, decay, uptake, and other mechanisms.

Subsurface Buffering Index. The subsurface buffering index is derived as a function of travel time from the source pixel to the receiving water, along a lateral groundwater flow path that follows the watertable slopes. Travel time is derived as the quotient of travel length and velocity:

$$\tau_{sub,i} = \frac{l_i}{V_{sub,i}} \qquad (11)$$

where l (m) is travel path distance for pixel i, and V_{sub} (m/s) is the subsurface runoff velocity for pixel i, computed with the Darcy equation:

$$V_{sub,i} = -K_i dz_i/dl * 1/p_i \qquad (12)$$

where K_i represents the pixel hydraulic conductivity (m/s), dz_i/dl represents the watertable gradient across the pixel, where z_i is pixel depth to watertable (m), and p is the pixel soil porosity. The $\tau_{sub,i}$ is set to 0 for all surface water pixels, which are considered receiving waters that have no buffering. The z_i term was determined as a function of runoff index, similar to the approach used by Endreny and Wood (1999):

$$z_i = \bar{z} - \frac{1}{f}(RI_{sub,i} - RI_{sub,avg}) \qquad (13)$$

where f parameterizes the decay of soil transmissivity with depth, and $\bar{z}$ represents the watershed average depth to watertable, which can be set using expert knowledge, calibration, or using the SSURGO dataset to determine the depth to the restrictive layer, as was done in this study. For the Onondaga Creek watershed, SSURGO reported watertable depths ranged from 36 to 201 cm, and saturated hydraulic conductivity ran-

ged from 1 to 25 cm/h. The subsurface buffering index is then calculated as the flow accumulation of travel times for all pixels in the subsurface dispersal area:

$$BI_{sub} = FA_{\tau_{sub,i}} \qquad (14)$$

where the $FA_{\tau_{sub,i}}$ algorithm uses flow directions derived from a negated watertable elevation map and a weighting grid of $\tau_{sub,i}$. The BI_{sub} calculation is based on longer travel times equating to greater chances for pollutant removal through a range of biophysical processes, such as particle filtration, decay, uptake, and other mechanisms.

CADA Model Sensitivity Tests

The CADA model predictions of N and P loading were tested for sensitivity to the spatial resolution of elevation and land cover inputs and the selection of EC and EMC values. Elevation and land cover are the data principal inputs for computation of the RI and BI terms in Equations (6), (7), (10), and (14). The spatial resolution of elevation and land cover was varied within a 4.2 ha sewershed in the City of Syracuse that had been surveyed using high-resolution airborne remote sensing to acquire elevation maps with 0.3 m horizontal resolution and 0.01 m vertical accuracy, and land cover maps at 0.3 m horizontal resolution classified into tree cover, pervious grass cover, and impervious cover. The 0.3 m resolution elevation and land cover inputs were resampled into coarser 1 and 10 m resolution products, representing resolutions that contain sub-grid heterogeneity within an urban landscape of crowned roads, curbs, herbaceous lawns, trees, sidewalks, and buildings. While the CADA runs required that SSURGO data be resampled into corresponding grids of 0.3, 1, and 10 m resolution, the initial SSURGO polygon areas were all larger than 100 m², and there was no loss of soil information moving between 0.3 and 10 m grid sizes. Using a fixed 10 m resolution for all inputs, the CADA model was also run with three different combinations of pixel NPS inputs, using EC values for all urban and rural pixels, EMC values for all urban and rural pixels, and EC values for rural pixels and EMC values for urban pixels.

RESULTS AND DISCUSSION

Urban and Rural, Surface and Subsurface Pollutant Loads

The spatial distribution and total watershed load of CADA predicted P and N values are highly sensi-

tive to the selection of pixel NPS inputs. The spatial distribution of weighted P and N loads for each pixel have heterogeneity in rural areas and more uniformity in urban areas when CADA was run with a combination of EC and EMC values (Figures 2A and 2D), while P and N loads were more uniform throughout the watershed when CADA was run with EC values (Figures 2B and 2E), and P and N loads were more heterogeneous when CADA was run with EMC values (Figures 2C and 2F). The CADA predicted watershed

P load was 14.9 tonnes/yr when estimated by the combination of EC and EMC values, slightly climbed to 15.6 tonnes/yr when estimated with only EC values, and significantly dropped to 6.7 tonnes/yr when estimated by only EMC values; the high and low P load range spanned 60% of the P load estimated by the load estimated by the combination of EC and EMC values. The CADA predicted watershed N load was 152.4 tonnes/yr when estimated by the combination of EC and EMC values, dropped to 138.9 tonnes/
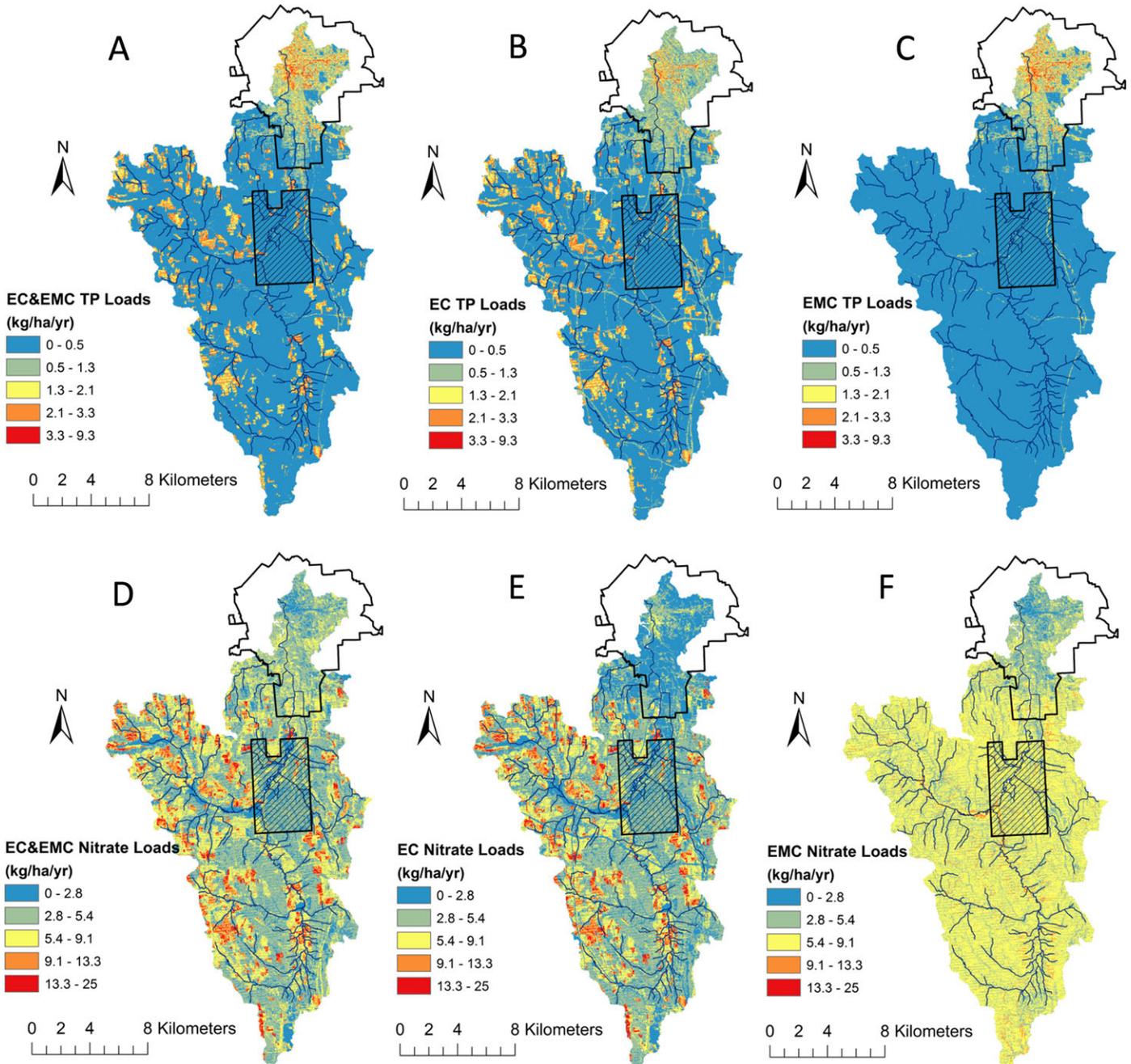
FIGURE 2. Demonstration of Using Export Coefficients and Event Mean Concentrations (EC&EMC), Only EC, and Only EMC to Determine Total Phosphorus (A-C) and Nitrate (D-F) Loads.

yr when estimated by only EC values, and climbed to 178.2 tonnes/yr when estimated by only EMC values; the high and low N load range spanned 25% of the N load estimated by the combination of EC and EMC values. For the CADA simulation using EC and EMC data, the 17.6% of the watershed area classified as developed land received EMC inputs, and EC inputs were applied to the remaining watershed area, and account for the majority of the P and N watershed loads. The 60% variation in CADA estimated P loads *vs.* a 25% variation in N loads is explained by the large variation in P EMC and EC inputs *vs.* N EMC and EC inputs (Table 1).

Use of EC input values for CADA estimates of NPS loads is recommended for rural land cover pixels, while EMC input values are recommended for NPS loads in urban land cover pixels. When EC inputs were used to estimate NPS loads on urban pixels (NLCD 21-24, Figure 1), the CADA model predicted fewer P loading hotspots in those urban areas than when hotspots were predicted using EMC inputs, where hotspots are defined as red colored pixels with a NPS P load >3.3 kg/ha/yr; this contrast in hotspots is illustrated in Figures 2B and 2C within the City of Syracuse polygon at the north end of the watershed. By contrast, the EC input values led to higher P estimates for rural agricultural pixels (NLCD 81 and 82, Figure 1) than estimated with EMC input values, which is noted by more yellow and orange colored pixels with a NPS P load >1.3 kg/ha/yr (see Figures 2B and 2C, to the south of the City of Syracuse, along Onondaga Creek tributaries). For CADA estimates of NPS N loads, the EC input values led to lower N loads on urban pixels than N loads estimated by the EMC input values, which is noted by fewer yellow colored pixels (>5.4 kg/ha/yr) in the City of Syracuse (Figures 2E and 2F). The EC input values led to higher estimates of NPS N loads for rural agricultural pixels than N loads estimated with EMC input values, noted by more orange and red pixels (>9.1 kg/ha/yr) along the headwater tributaries. Due to the small variation in impervious cover and the associated runoff coefficient, R_v, there was little spatial variation in CADA estimated P and N loads for rural areas when EMC input values were used (see large area in blue color with 0-0.5 kg/ha/yr of P in Figure 2E, and large area in yellow color with 5.4-9.1 kg/ha/yr of N in Figure 2F). By contrast, when EC input values were used, loading was not sensitive to the R_v, but instead correlated strongly with land cover classes; note the greater heterogeneity with EC-based loads than EMC-based loads in the southern watershed (Figure 2E *vs*. 2F). The CADA model estimates of NPS N and P loads in this case were more sensitive to EMC and EC inputs than to buffering processes in the runoff distribution area.

The accuracy of CADA-predicted NPS loads was constrained by the first-order and parsimonious nature of the model equations and by our choice to not calibrate the model inputs of EC or EMC or vary inputs across years. In a test of accuracy, the CADA predicted P load using a combination of EC and EMC inputs was 25% above the observed 11.16 tonnes/yr load, while the CADA predicted N load was 6.6% below the observed 162.5 tonnes/yr load. These observed loads represent a six year average, obtained using water quality and discharge data collected by the U.S. Geological Survey (USGS) at the Onondaga Creek Spencer Street USGS gage between October 1, 1997 and September 30, 2003 as part of the Onondaga County Ambient Monitoring Program (Coon and Reddy, 2008). The USGS used these observed loads to derive EC input values, which were within the range provided by the national datasets (Table 1). While most watersheds will not have observed loads to calibrate the EC and EMC datasets, the CADA model remains a useful tool for estimating a range of possible NPS loads. Ranges of loads were also calculated, using the lowest and highest EC values from Table 1 combined with the 10th and 90th percentiles of EMC values Equations (4) and (5), respectively. The results showed that for the lowest values scenario, we observed 59.9 and 3.3 tonnes/year loads for N and P, respectively. The highest value scenario resulted in 313.3 tonnes/year and 108.1 tonnes/year loads for N and P, respectively. These ranges provide bounds for minimum and maximum loading expected over different years. Based on the Onondaga Lake Ambient Monitoring Program, managed through the Onondaga County Department of Water Environment Protection, the range of loading values from Onondaga Creek to Onondaga Lake is 140-220 tonnes/year for nitrate and 11-25 tonnes/year for phosphorus. We recommend using the model with a range of feasible input values for each pixel, varying EC and EMC (see Table 1 ranges), as well as varying R_v, R, n, T, and other terms in order to capture input uncertainty and provide an upper and lower bound for estimated NPS loads.

Runoff Indices — Surface and Subsurface

The spatial distribution of the surface runoff index and subsurface runoff index reflect the impact of contributing areas to the CADA estimated NPS loads. Both runoff indices use contributing area and as a result they generally reflect an increasing likelihood for runoff with proximity to the stream network; however, there are regions where RI_{surf} varies significantly from RI_{sub}. In the urban areas, such as those in the northern end of the Onondaga Creek water-

shed, the RI_{surf} tended toward higher values (blue colored pixels, Figure 3A), while the RI_{sub} had lower values (green and yellow colored pixels, Figure 3B), which captures the effect of imperviousness partitioning precipitation into overland flow. By contrast, rural land cover will have greater perviousness and partition precipitation into subsurface flow, generating relatively low RI_{surf} values (see yellow to orange color pixels in the rural southern watershed region, Figure 3A) and relatively high RI_{sub} values (see green colored higher pixels in the rural southern watershed region, Figure 3B). The spatial differences between RI_{sub} and RI_{surf} are also due to the RI_{sub} calculation using soil transmissivity and watertable elevation data, while the RI_{surf} used surface elevation data. The mean RI_{sub} value was 8.4, 50% higher, in natural log space, than the mean RI_{surf} value of 5.6. The significantly larger RI_{sub} value is attributed to the much larger watershed area in pervious cover, estimated at 94%, and as a result the Onondaga Creek watershed RI_{sub} values correspond with reported ranges for neighboring, predominantly rural, Finger Lakes region catchments (e.g., Anderson *et al.*, 2015).

Buffer Indices — Surface and Subsurface

The spatial distribution of surface runoff velocities (Figure 4A) and subsurface runoff velocities (Figure 4B) largely regulate the corresponding BI_{surf} and BI_{sub}. Road networks have the lowest Manning n roughness values, which create a signature pattern of high surface velocities where roads contrast with nonroad pixels (see linear bands of red colored pixels in the mid to southern sections of the watershed, and swaths in the City of Syracuse in Figure 4A). The predicted surface velocities ranged from 0.0002 to 1.7 m/s, with the upper limits agreeing with values expected for runoff over roads. The predicted subsurface velocities were two orders of magnitude lower than surface velocities, and correspond to residence times of days to years for flow through the watershed. Slope had a large influence on velocity, and in a west to east transect across the urban area in the north of the watershed, the surface velocities are at their lowest in the center of the transect corresponding to the urban floodplain despite a dense network of roads (see blue colored pixels bounded by red colored pixels in Figure 4A). By contrast, the subsurface velocities are not influenced by roads and are relatively low values in the northern urban area; they are highest in the mid to southern sections of the watershed along the steep valley walls bounding Onondaga Creek (Figure 4B); the valley is glacially carved and has classic U-shaped valley walls.

The BI_{surf} and BI_{sub} values were often highest at the two geographic extremes of watershed ridges and valleys or floodplains (see Figures 5A and 5B). The ridges corresponded to the greatest flow path distances to the receiving waters, and hence relatively long travel times, while the valleys and floodplains corresponded to relatively flat slopes and long travel times. In addition to flow path length and slope, the BI_{surf} is also affected by the vegetative cover in the
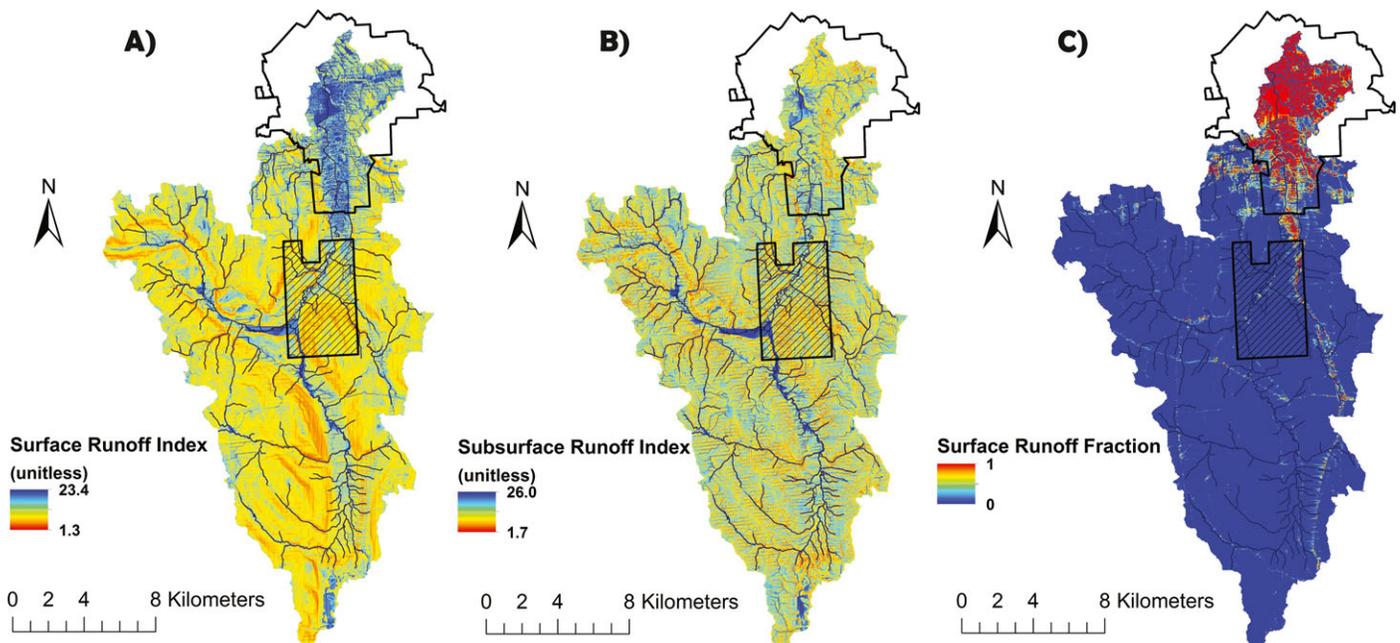
FIGURE 3. Surface (A) and Subsurface (B) Runoff Indices and Percentage of Surface Runoff (C).

dispersal area flow path. When urban stormwater management involves efforts to slow down surface runoff, planting higher roughness land cover types in the dispersal area can increase the likelihood for pollutant buffering and reduce NPS loading. In efforts to reduce subsurface loading, management options may include creation of higher transmissivity preferential flow paths to guide runoff into treatment cells, perhaps with aeration or biological treatment, as envisioned by Vaux (1968) for improving aquatic conditions.

Impacts of Elevation and Land Cover Spatial Resolution

The CADA NPS model predictions of P and N loading hotspots were highly sensitive to the spatial resolution of elevation and land cover. The outputs of P and N hotspots predicted with 0.3 m and 1 m horizontal resolution inputs captured the pattern of roads and houses in the 14 ha sewershed (Figures 6A and 6B), while the 10 m resolution did not capture road patterns and only weakly captured houses (Figure 6C). The even coarser 30 m spatial resolution inputs from NLCD are likely the most common resolution for land cover data, and clearly would not capture spatial patterns of the urban landscape missed by the 10 m data. Maps of predicted NPS loading can guide managers toward watershed areas in need of runoff control measures, and to capture the influence

of urban landscape features such as roads and houses, the 1 m or finer resolution data are recommended for CADA simulations. The confidence in the CADA model predicted hotspots, defined as disproportionately high P or N loads, and their opposite, coldspots, can be quantified with the Getis-Ord statistic at values of 95% (Table 3). The Getis-Ord statistic, for both hotspots and coldspots, differentiates statistically significant clusters of high or low valued pixels from pixel clusters that are randomly organized (Getis-Ord <95%). The patterns of Getis-Ord hotspots and coldspots corresponded to the road network within the 14 ha watershed, noted in the simulation using 0.3 m resolution input data (Figure 6D), but less so for the 1 and 10 m resolution simulations (Figures 6E and 6F). At a 0.3 m resolution, a total of 49.7% of the sewershed fell within hotspots or coldspots with >95% confidence; the percentage drops down to 28% and 3.8% for resolutions of 1 and 10 m, respectively. This trend is explained by the coarser inputs causing a blending of otherwise distinct boundaries between land cover, thereby generating fewer differences in pixel P and N loading values. With finer input resolution, there is more opportunity for the CADA NPS model to confidently predict the spatial variation in P and N hotspot and coldspot clusters.

The pixel NPS loads also changed significantly with the resolution of the CADA input data of elevation and land cover. The CADA predicted a maximum pixel N load of 11.7 kg/ha/yr for the 0.3 m resolution
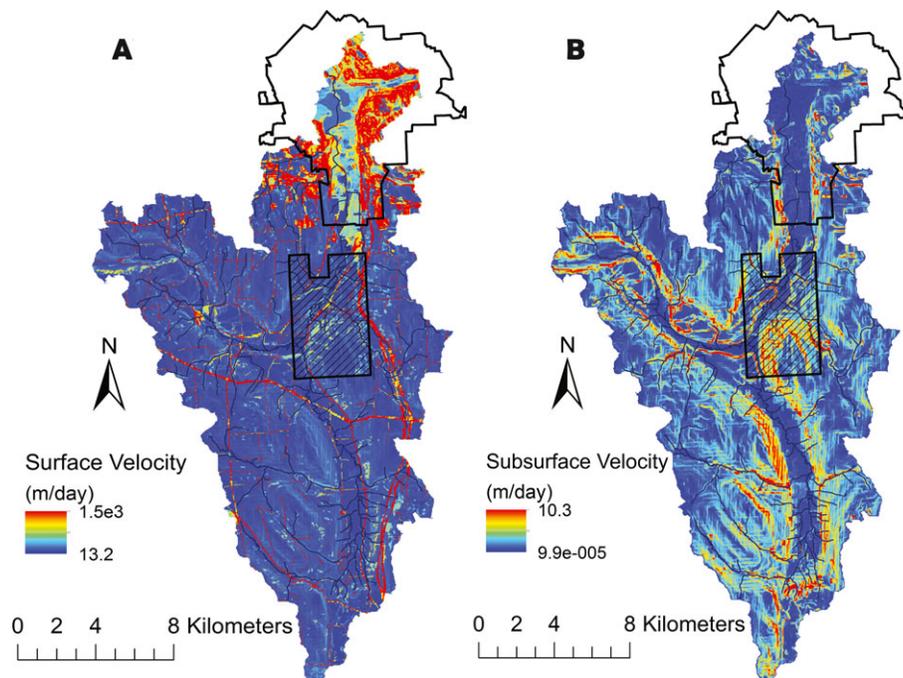
FIGURE 4. Surface (A) and Subsurface Velocities (B).
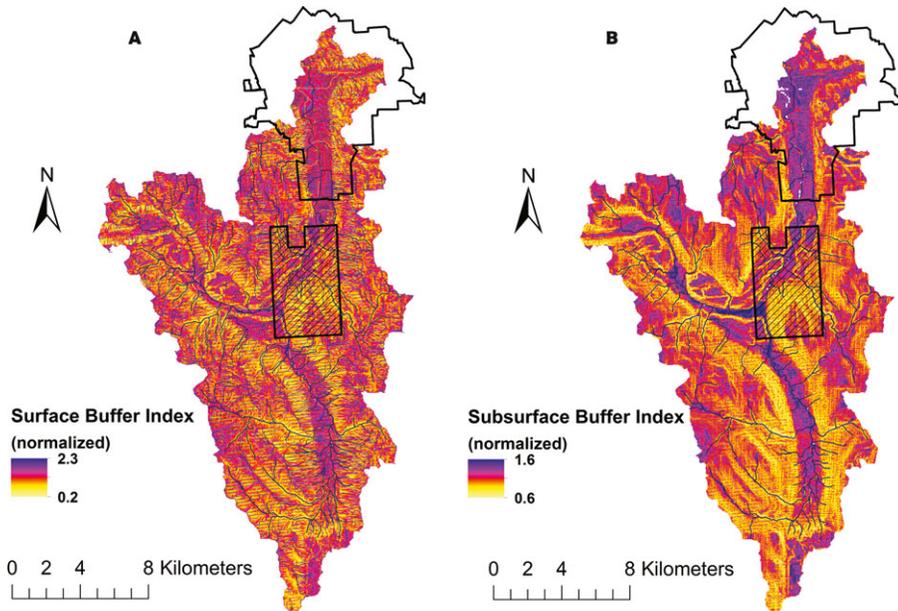
FIGURE 5. Surface (A) and Subsurface (B) Buffering Indices.
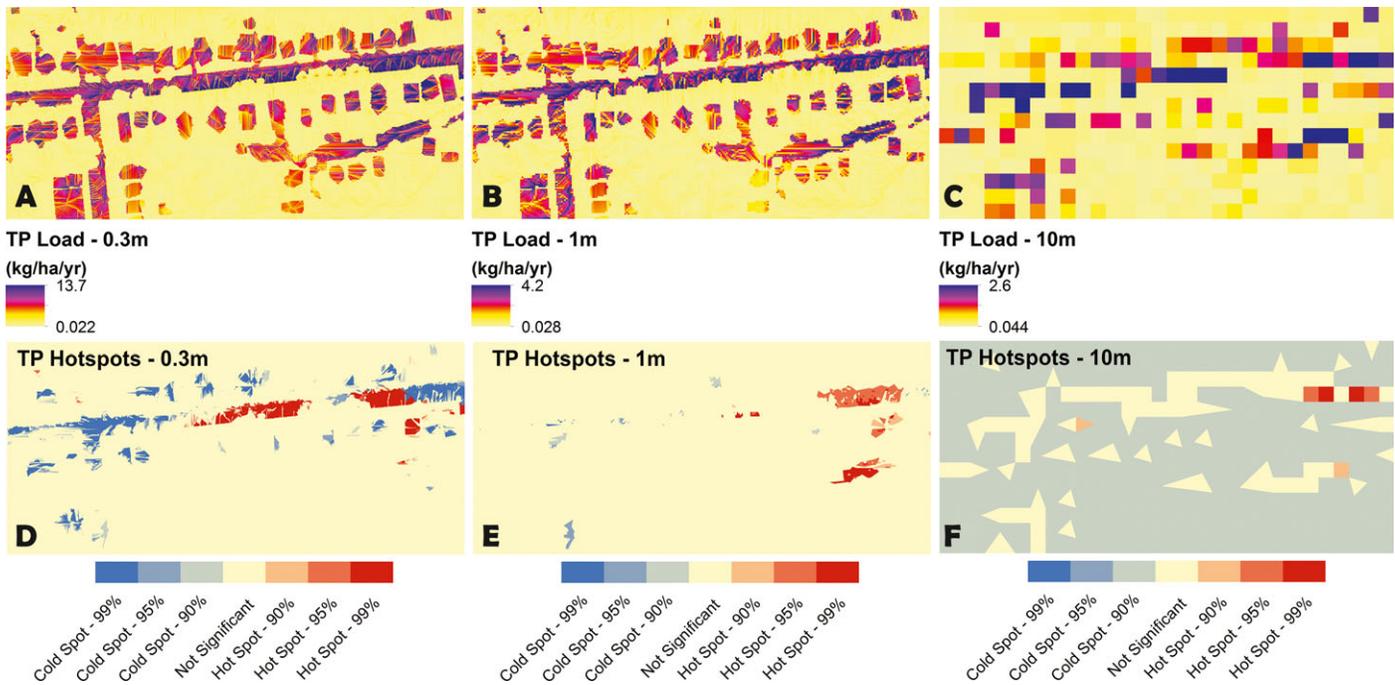
FIGURE 6. TP Sensitivity and Getis-Ord* Hotspot Analysis.

simulation, and this maximum pixel N load decreased by 35% to 7.6 kg/ha/yr for the 10 m resolution simulation (Figures 7A and 7C). As elevation and land cover input resolution coarsened beyond 1 m, there was a reduction in maximum pixel NPS load values and a lowering of the Getis-Ord confidence in the hotspots and coldspots pixel clusters. The CADA model predictions of watershed NPS load, defined as the sum of all pixel NPS loads, had less sensitivity to the spatial resolution of elevation and land cover in the sewershed simulations. Despite pixel load sensitivity for CADA simulations of P, the watershed P load only varied by 0.7% between the simulations using 0.3 and 10 m inputs. The 0.3 m resolution inputs of elevation and land cover generated watershed P loads of 1.51 kg/yr, while the 10 m resolution inputs gener-

TABLE 3. Percentage of Sewershed Falling in Hotspots and Cold-spots above 95% Confidence.

Resolution (m)	Percent in 95-99% Coldspot		Percent in 95-99% Hotspot	
	Nitrate	TP	Nitrate	TP
0.3	29.4	4.4	20.3	2.2
1	14.8	0.2	13.2	1.8
10	0.0	0.0	3.8	1.3

ated 0.7% larger watershed P loads. Despite the sensitivity of maximum pixel NPS loads to input resolution, the watershed N load from the sewershed did not vary significantly with input resolution. The 0.3 m simulation generated a CADA predicted watershed N load of 16.93 kg/yr, while the 1 m and 10 m simulations generated watershed N loads within 1%, at 16.72 kg/yr and 16.53 kg/yr, respectively.

The CADA predicted pixel P and N loads (Figures 2A and 2D) were based on the RI_{surf}, RI_{sub}, BI_{surf}, and BI_{sub} values, which are regulated by Manning and Darcy velocity Equations (9) and (12) and very sensitive to slope values calculated by the ArcGIS method. For each pixel, the CADA model calculated the slopes to each of the eight neighboring pixels, and selected the steepest slope for the velocity calculations, but this may not necessarily be the actual flow path for runoff in urban areas where sub-grid elevation heterogeneity such as curbs and gutters and riffles may regulate flow slopes. In land cover classes designated as urban, the CADA slope

calculations were constrained to a maximum slope of 6%, in order to ensure road slopes are within the recommended maximum (American Association of State Highway and Transportation, 2011), and runoff velocities along roads were not excessively rapid. In cases where higher slopes do exist, flow would likely become unsteady and depart from Manning assumptions, which would require alternative, perhaps hydraulic-based, estimates for velocity.

SUMMARY AND CONCLUSIONS

This research enhanced the CADA NPS model to achieve three goals in watershed simulation of nutrient hotspot mapping: (1) flexibility to use EC, EMC, or other NPS loading data for N or P loads; (2) representation of impervious and pervious runoff paths in the contributing area; and (3) representation of surface and subsurface buffer paths in the dispersal area. These updates are critical for the co-management of P and N, which often occur in the surface and subsurface runoff flowpaths at different proportions. Historically, freshwater systems have been assumed P limited, due to the abundance of N in freshwater via N fixing cyanobacteria (Conley et al., 2009). Therefore, many freshwater management efforts have focused more on P than N. However, the urban biogeochemistry of complex social-infrastruc-
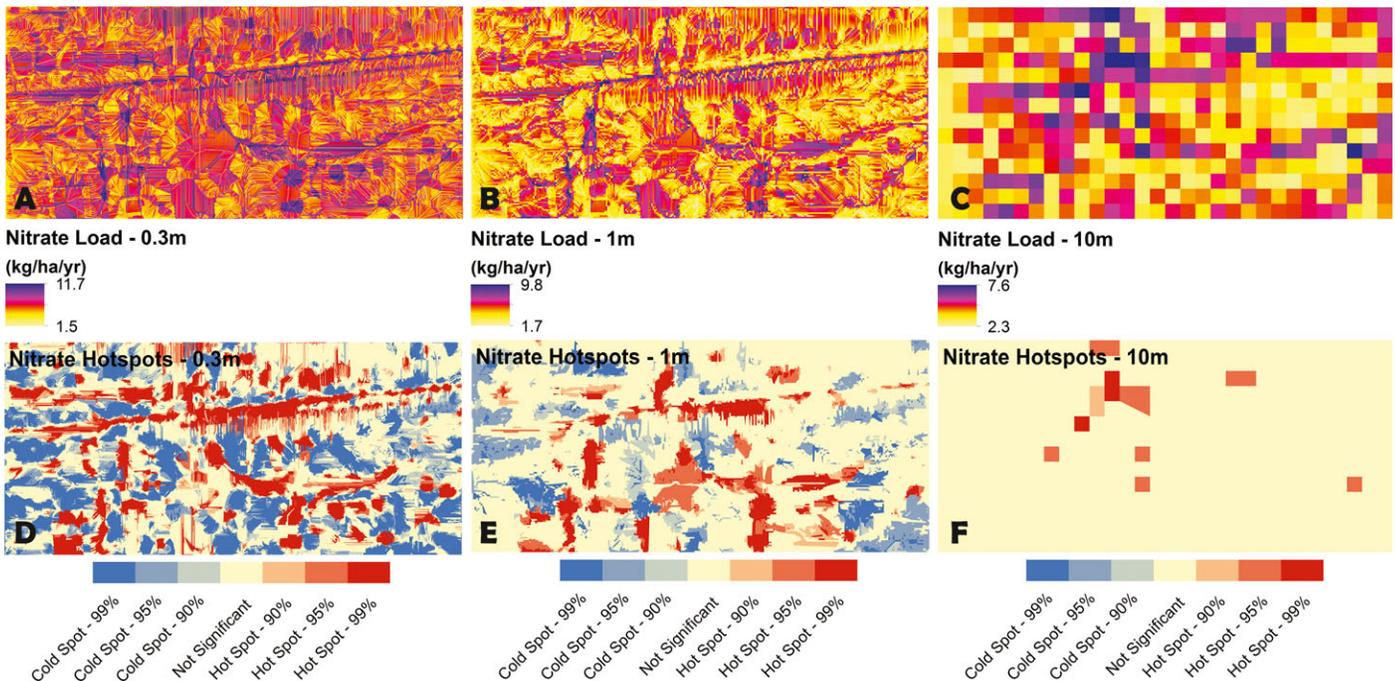
FIGURE 7. Nitrate Sensitivity and Getis-Ord* Hotspot Analysis.

ture-environmental interactions result in elevated nutrient concentrations along accelerated flow paths with a high level of apparently random individual decisions affecting receiving water quality (Kaye *et al.*, 2006). Nutrient loads to urban receiving waters have been shown to have lower N:P ratios, which results in N as the limiting nutrient to eutrophication (Howarth and Marino, 2006). Coastal receiving waters are N limited (Nixon, 1995), and urban and rural drainage with elevated N loads, from sanitary waste, agricultural runoff, and other sources, also accelerates eutrophication in coastal systems. The enhanced CADA NPS model allows for simulation of urban and rural pollutant sources from mixed land use watersheds, and the surface and subsurface runoff pathways connecting this pollution with CADA processes, providing an important management tool for inland and coastal communities.

The enhanced CADA NPS model provides spatial maps of the weighted EC and EMC hotspots and coldspots contributing to watershed nutrient loads, and allows managers to differentiate between interventions that reduce surface transported pollutants, such as particulate phosphorus, from interventions targeting subsurface transported pollutants, such as dissolved nitrate. While the spatial maps provide a first order estimate of loading hotspots, they do not represent the uncertainty in the predictions and users should run CADA NPS with low and high values of EC and EMC inputs to simulate a range of possible NPS loads, which are more likely to capture the observed loading value for the pixel and the watershed (Endreny and Wood, 2003). One proposed update for the CADA NPS model includes simulation of denitrification as a nutrient removal process, to better represent the spatial dependency between organic matter, moisture, and losses of nitrate in the landscape (Sudduth *et al.*, 2013). Another proposed update for the CADA NPS model is to provide storm-based temporal variation in load estimates, allowing for managers to examine loading sensitivity to storm intensity, which is sensitive to climate change, and where raindrop splash intensity and pollutant displacement might be managed by vegetative cover. Each of these proposed updates would strive to keep CADA NPS a parsimonious first order model that uses available datasets, and facilitates its use in many watershed projects evaluating how changes in land cover might affect the distribution of nutrients in the landscape and loads to receiving waters.

LITERATURE CITED

American Association of State Highway and Transportation, 2011. A Policy on Geometric Design of Highways and Streets, 2011. AASHTO, Washington, D.C.

Anderson, T.R., P.M. Groffman, and M.T. Walter, 2015. Using a Soil Topographic Index to Distribute Denitrification Fluxes across a Northeastern Headwater Catchment. Journal of Hydrology 522, 123-134, DOI: 10.1016/j.jhydrol.2014.12.043.

Bettez, N.D. and P.M. Groffman, 2012. Denitrification Potential in Stormwater Control Structures and Natural Riparian Zones in an Urban Landscape. Environmental Science & Technology 46 (20):10909-10917, DOI: 10.1021/es301409z.

Beven, K.J. and M.J. Kirkby, 1979. A Physically Based, Variable Contributing Area Model of Basin Hydrology. Hydrological Sciences Bulletin 24(1):43-69. DOI: 10.1080/02626667909491834.

Borah, D.K. and M. Bera, 2004. Watershed-Scale Hydrologic and Nonpoint-Source Pollution Models: Review of Applications. Transactions of the ASAE 47:789-803.

Carpenter, S.R., N.F. Caraco, D.L. Correll, R.W. Howarth, A.N. Sharpley, and V.H. Smith, 1998. Nonpoint Pollution of Surface Waters with Phosphorus and Nitrogen. Ecological Applications 8(3):559-568, DOI: 10.1890/1051-0761(1998)008[0559:NPOSWW] 2.0.CO;2.

Conley, D.J., H.W. Paerl, R.W. Howarth, D.F. Boesch, S.P. Seitzinger, K.E. Havens, and G.E. Likens, 2009. Controlling Eutrophication: Nitrogen and Phosphorus. Science 323(5917):1014-1015, DOI: 10.1126/science.1167755.

Coon, W.F. and J.E. Reddy, 2008. Hydrologic and Water-Quality Characterization and Modeling of the Onondaga Lake Basin, Onondaga County. U.S. Geological Survey, New York City, New York.

Donigian, A.S., B.R. Bicknell, and J.C. Imhoff, 1995. Hydrological Simulation Program - Fortran (HSPF). *In*: Computer Models of Watershed Hydrology, V.P. Singh (Editor). WRP, Highlands Ranch, Colorado, USA, pp. 395-442.

Douglas-Mankin, K.R., R. Srinivasan, and J.G. Arnold, 2010. Soil and Water Assessment Tool (SWAT) Model: Current Developments and Applications. Transactions of the ASABE 53(5):1423-1431.

Endreny, T.A. and E.F. Wood, 1999. Distributed Watershed Modeling of Design Storms to Identify Nonpoint Source Loading Areas. Journal of Environment Quality 28(2):388, DOI: 10.2134/jeq1999.00472425002800020004x.

Endreny, T.A. and E.F. Wood, 2003. Watershed Weighting of Export Coefficients to Map Critical Phosphorous Loading Areas. Journal of the American Water Resources Association 39(1):165-181, DOI: 10.1111/j.1752-1688.2003.tb01569.x.

Engman, E., 1986. Roughness Coefficients for Routing Surface Runoff. Journal of Irrigation and Drainage Engineering 112 (1):39-53, DOI: 10.1061/(ASCE)0733-9437(1986)112:1(39).

Fisher, P., R.J. Abrahart, and W. Herbinger, 1997. The Sensitivity of Two Distributed Non-Point Source Pollution Models to the Spatial Arrangement of the Landscape. Hydrological Processes 11(3):241-252, DOI: 10.1002/(SICI)1099-1085(19970315) 11:3 < 241::AID-HYP438 > 3.0.CO;2-T.

Howarth, R.W. and R. Marino, 2006. Nitrogen as the Limiting Nutrient for Eutrophication in Coastal Marine Ecosystems:

Evolving Views over Three Decades. Limnology and Oceanography 51(1_part_2):364-376, DOI: 10.4319/lo.2006.51.1_-part_2.0364.

Huber, W.C., 1995. EPA Storm Water Management Model (SWMM). *In*: Computer Models of Watershed Hydrology, V.P. Singh (Editor). WRP, Highlands Ranch, Colorado, USA, pp. 783-808.

Kaushal, S.S., P.M. Groffman, L.E. Band, E.M. Elliott, C.A. Shields, and C. Kendall, 2011. Tracking Nonpoint Source Nitrogen Pollution in Human-Impacted Watersheds. Environmental Science & Technology 45(19):8225-8232, DOI: 10.1021/es200779e.

Kaye, J.P., P.M. Grimm, N.B. Baker, and R.V. Pouyat, 2006. A Distinct Urban Biogeochemistry? Trends in Ecology & Evolution 21 (4):192-199, DOI: 10.1016/j.tree.2005.12.006.

Lewis, W.M., W.A. Wurtsbaugh, and H.W. Paerl, 2011. Rationale for Control of Anthropogenic Nitrogen and Phosphorus to Reduce Eutrophication of Inland Waters. Environmental Science & Technology 45(24):10300-10305, DOI: 10.1021/es202401p.

Nixon, S.W., 1995. Coastal Marine Eutrophication: A Definition, Social Causes, and Future Concerns. Ophelia 41(1):199-219, DOI: 10.1080/00785236.1995.10422044.

Reckhow, K.H., Beaulac M.N., and J.T. Simpson, 1980. Modeling Phosphorus Loading and Lake Response Under Uncertainty: A Manual and Compilation of Export Coefficients (US EPA 440/5-80-011). US Environmental Protection Agency, Washington, D.C.

Reckhow, K.H. and J.T. Simpson, 1980. A Procedure Using Modeling and Error Analysis for the Prediction of Lake Phosphorus Concentration from Land Use Information. Canadian Journal of Fisheries and Aquatic Sciences 37(9):1439-1448, DOI: 10.1139/f80-184.

Schueler, T.R., 1987. Controlling Urban Runoff: A Practical Manual for Planning and Designing Urban BMPs. Metropolitan Washington Council of Governments, Washington, D.C.

Sivapalan, M., K. Beven, and E.F. Wood, 1987. On Hydrologic Similarity: 2. A Scaled Model of Storm Runoff Production. Water Resources Research 23(12):2266-2278, DOI: 10.1029/WR023i012p02266.

Smith, V.H. and D.W. Schindler, 2009. Eutrophication Science: Where Do We Go from Here? Trends in Ecology & Evolution 24 (4):201-207, DOI: 10.1016/j.tree.2008.11.009.

Sudduth, E.B., S.S. Perakis, and E.S. Bernhardt, 2013. Nitrate in Watersheds: Straight from Soils to Streams? Journal of Geophysical Research: Biogeosciences 118(1):291-302, DOI: 10.1002/jgrg.20030.

Tague, C.L. and L.E. Band, 2004. RHESSys: Regional Hydro-Ecologic Simulation System—An Object-Oriented Approach to Spatially Distributed Modeling of Carbon, Water, and Nutrient Cycling. Earth Interactions 8(1):1-42.

USEPA (U.S. Environmental Protection Agency), 1983. Results of the Nationwide Urban Runoff Program: Volume 1 - Final Report. Water Planning Division, Washington, D.C.

Vaux, W.G., 1968. Intergravel Flow and Interchange of Water in a Streambed. Fishery Bulletin 66(3):479-489.

Wang, J., T.A. Endreny, and D.J. Nowak, 2008. Mechanistic Simulation of Tree Effects in an Urban Water Balance Model. Journal of the American Water Resources Association 44(1):75-85, DOI: 10.1111/j.1752-1688.2007.00139.x.

Wurbs, R.A. and W.P. James, 2002. Water Resources Engineering (First Edition). Prentice Hall, Upper Saddle River, New Jersey.

Young, R.A., C.A. Onstad, D.D. Bosch, and W.P. Anderson, 1989. AGNPS: A Nonpoint-Source Pollution Model for Evaluating Agricultural Watersheds. Journal of Soil and Water Conservation 44(2):168-173.

Zhang, T., P.A. Soranno, K.S. Cheruvelil, D.B. Kramer, M.T. Bremigan, and A. Ligmann-Zielinska, 2012. Evaluating the Effects of Upstream Lakes and Wetlands on Lake Phosphorus Concentrations Using a Spatially-Explicit Model. Landscape Ecology 27(7):1015-1030, DOI: 10.1007/s10980-012-9762-z.